compact nature of seed-derived calli in indica varieties and problems associated with it can be circumvented by direct bombardment of rachilla-derived callus. The increased efficiency and rapidity of selection of transformants coupled with its superior regeneration makes the rachilla a potential explant source for tissue culture as well as transformation studies. Further, for protoplast-mediated gene transfer, rachilla-derived calli have an additional advantage as the time required for establishing the uniform embryogenic suspension cultures is reduced. With the availability of an additional source of embryogenic callus and the attendant advantages, our efforts are focussed on further enhancing the frequency of callus induction from rachilla for use in genetic transformation either through direct bombardment or development of embryogenic cell suspensions to isolate protoplasts for PEG-mediated transformation or electroporation. Because of its superior regeneration potential, rachilla callus can also be used for maintenance and multiplication of male sterile lines in plant breeding programmes.

1. Zhang, S., Chen, L., Qu, R., Marmey, P., Beachy, R. and Faquet, C., *Plant Cell Rep.*, 1996, **15**, 465–469.
2. Jain, R. K., Jain, S., Wang, B. and Wu, R., *Plant Cell Rep.*, 1996, **15**, 963–968.
3. Christou, P., in *Rice Biotechnology and Genetic Engineering*, Technomic Publishing Co. Inc., USA, 1994, pp. 45–93.
4. Murashige, T. and Skoog, F., *Physiol. Plant*, 1962, **15**, 473–497.
5. Chu, C. C., Wang, C. C., Sun, C. S., Hsu, S. C., Yin, K. C., Chu, C. Y. and Bi, F. Y., *Sci. Sinica.*, 1975, **18**, 659–668.
6. Sivamani, E., Shen, P., Opalka, N., Beachy, R. N. and Fauquet, C. M., *Plant Cell Rep.*, 1996, **15**, 322–327.
7. Chen, T. H., Lam, L. and Chen, S. C., *Plant Cell Tiss. Organ Cult.*, 1985, **4**, 51–54.
8. Wang, M. S., Zapata, F. J. and De Castro, D. C., *Plant Cell Rep.*, 1987, **6**, 294–296.
9. Ling, D. H. and Komamine, A., *J. Tropical Subtropical Bot.*, 1994, **2**, 70–78.
10. Poonspaya, P., Nabors, M. W., Wright, K. and Vajrabhaya, M., *Plant Cell Tiss. Organ Cult.*, 1989, **16**, 175–186.
11. Jain, R. K., Jain, S. and Wu, R., *Plant Cell Rep.*, 1996, **15**, 449–454.

ACKNOWLEDGEMENTS. The support from The Rockefeller Foundation, New York, through a Project grant (RF92003 #129) to the Directorate of Rice Research is gratefully acknowledged.

Received 28 December 1997; revised accepted 26 March 1998

A^+–C Mismatched base-pairing in DNA

Sukesh R. Bhaumik and Kandala V. R. Chary*

Department of Chemical Sciences, Tata Institute of Fundamental Research, Homi Bhabha Road, Mumbai 400 005, India

The structural aspects of an antiparallel DNA duplex with A^+–C mismatched base-pair by molecular dynamics calculations are discussed. The A^+–C mismatched base-pair which has been characterized by NMR with two hydrogen bonds namely, $A^+(6NH_2)$–C(3N) and $A^+(1NH)$–C(2O), fits into B-form duplex with little distortion in the pyrimidine strand. A in the A^+–C mispair is efficiently stacked to the flanking purine bases. Such efficient purine–purine stacking provides extra stabilization to this mismatched base-pair. On the other hand, C in the mispair is displaced from the helix axis while adjacent T (i.e. T7) is slightly off because of the enhanced base-pair twist. This supports the experimental observation of unusual chemical shifts for the H5 and H6 protons belonging to the C of the A^+–C mismatched base-pair.

MISMATCHES in DNA can arise during replication, and in genetic recombination[1–4]. If they are not corrected, the mismatches may lead to point mutations in subsequent replication. There have been several investigations by X-ray and solution NMR on purine–purine (A–A, A–G, A–I and G–G), purine–pyrimidine (A–C and G–T) and pyrimidine–pyrimidine (C–C, T–T and T–C) mismatches in oligonucleotides[5–28]. The studies on A–C mismatched base-pair support that the wobble pair is stabilized by $A(6NH_2)$–C(3N) hydrogen bond. Based on the observed short nitrogen–carbon distance in the crystal, it was suggested that the A–C mismatch pair is stabilized by a second hydrogen bond involving 1NH of protonated A and 2CO of C. Though pKa for the protonation of A in the free base is approximately 4, it was suggested to be higher when A basepairs with C in a DNA duplex[25–28].

5′TGAGGAAAGAAGGT3′
3′CCTTCTTTCCTC 5′
M1

In a recent NMR study on the molecular system M1, we have characterized the formation of a stable antiparallel duplex at neutral pH with three mismatched base-pairs, A^+–C, G–T and T–C (ref. 29). The study provided the first evidence for the protonation of A(N1) site at neutral pH leading to the formation of A^+–C mismatched base-pair with two hydrogen bonds, $A^+(1NH)$–C(2O) and $A^+(6NH_2)$–C(3N).

*For correspondence. (e-mail: Chary@tifrvax.tifr.res.in)

$5'A_1\,GAAG_5 3'$
$3'T_{10}CCTC_6 5'$
M2

In this communication, we discuss the structural aspects of an antiparallel DNA duplex with A^+–C mismatched base-pair by molecular dynamics calculations. In this endeavour, a computer graphics molecular model of five base-pair stretch of an unusual duplex, M2, was constructed with A^+–C mismatch in the middle and two Watson–Crick base-pairs on either side. Molecular dynamics simulation and energy minimization were performed on the generated structure based on experimental NMR constraints.

Molecular dynamics simulations were performed with the DISCOVER (MSI, San Diego, CA). A time step of 1 fs was used. Initial random velocities were assigned keeping in accord with a Maxwell–Boltzmann distribution. To obtain the starting structure, an initial steepest decent minimization of 100 steps was performed on the initial structure followed by conjugate gradient minimization of 1000 steps. This was followed by 200 ps of molecular dynamics at 300 K and another 1000 steps of conjugate gradient minimization.

The protocol for molecular dynamics studies is as follows. Initial random velocities were assigned with a Maxwell–Boltzmann distribution for a temperature of 500 K. Then the molecule was cooled to 300 K in steps of 50 K. After each temperature step, the system was allowed to equilibriate for 10 ps. 200 ps molecular dynamics trajectory was then generated at 300 K, and analysed.

AMBER force field was used to calculate the energy of the system. Electrostatic interactions were calculated using Coulomb's law with point charges. Distance-dependent dielectric constant of '1*r' was used. van der Waals contributions were calculated with a 6–12 Lennard–Jones potential.

An initial B-DNA duplex structure (M2) with the sequence of individual strands as 5′–d–$A_1G_2A_3A_4G_5$ and 5′–d–$C_6T_7C_8C_9T_{10}$ was generated using the molecular modelling package INSIGHT-II (MSI, San Diego, CA) on Iris (Indigo 2) workstation. A3 was protonated at N_1 atom. This was done by changing the hybridization of N_1 from sp^2 to sp^{2+} followed by the formation of partial double bonds between N_1 and C_6, and C_6 and N_6 atoms of A3. The A^+ thus obtained was recognized by DISCOVER. However, charges on A^+ are not defined in AMBER. Thus, in the first approximation, we have assigned the charges of $N1^+$–H atoms of A^+ to be the same as for $N3^+$–H atoms of C^+. The charges for the other atoms of A^+ were kept fixed.

The 5′ and 3′-terminals were capped by –OH groups. All hydrogen atoms were represented explicitly. The hydrogen bonding schematics for various base-pairs have been derived from the knowledge of the chemical shifts of the exchangeable imino and amino proton resonances in the ^1H spectrum[29] and their nOe correlations with other intra– and inter–strand base protons. The base-pairs, A1:T10, G2:C9, A4:T7 and G5:C6 are essentially held together by standard Watson–Crick hydrogen bonding as derived from the NMR data. The A^+–C base-pairing has been characterized with two hydrogen bonds ($A^+(6NH_2)$–C(3N) and $A^+(1NH)$–C(2O)) as shown in Figure 1. This is based on the observation of $A^+(1NH)$ proton resonance in the ^1H spectrum, which has been assigned from the observation of intranucleotide NOESY cross peak to A(H2) proton. This was further supported from the observation of the nOes such as A3(H2) to G2(1NH), A3(H8) to G2(H8), A3(H2) to A4(H2) and A3(H8) to A4(H8)[29].

Molecular dynamics simulation and energy minimization calculations were performed on the generated structure with the interproton distance constraints (32 in total; 25 involving exchangeable protons and 7 involving nonexchangeable protons) obtained from NMR data. All base pairs showed evidence of hydrogen bonding, the heavy atoms in the Watson–Crick were restrained in the range 2.8–3.25 Å. Tight restraints were also used that correspond to the strong nOes observed between A(H2) and 3NH of the paired T (2.4–3.0 Å), and the analogous G(1NH) and C($4NH_2$; HB) (2.4–3.0 Å). Other distances involving exchangeable protons were restrained much more weakly, with typical limits of ±0.5 Å. This allows for leakage process by exchange with solvent. The upper limit is the more important one in these instances, as the sequential nOes are limited at the lower end by the van der Waals contacts between neighbouring base pairs. The nOe distances involving sequential and non-exchangeable H8–H8 and H6–H6 protons along purine and pyrimidine strands, respectively, were restrained in the range 3.40–4.60 Å, while A^+3(H2)–A4(H2) distance was restrained in the range 3.60–4.00 Å.

Two hundred structures were collected at 1 ps interval along the molecular dynamics trajectory and they were energy minimized. Figure 2 shows the plot of energy vs. different structures thus obtained. As seen in Figure

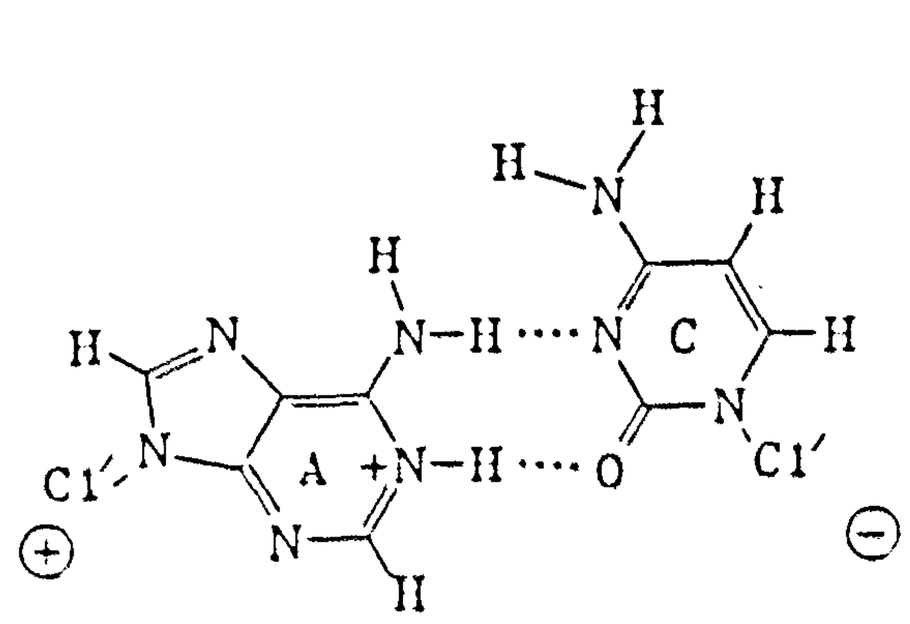

Figure 1. Hydrogen-bonding scheme for A^+–C mismatch base-pair.

2, the structure at 195 ps on the simulation trajectory has the lowest energy. However, there are 10 other structures (at 93, 106, 107, 110, 120, 139, 142, 153, 165 and 189 ps) which lie within 2.5 kcals above the structure at 195 ps (Figure 2) and have no structural diversity as discussed later. Hence, for discussion purpose, the structural aspects of the 195 ps structure have been used. The stereo view of the 195 ps structure is shown in Figure 3. A3 is efficiently stacked to the flanking bases, G2 and A4 as shown in Figure 4. Such stacking should give rise to the following nOe interactions: A3(H8) to G2(H8), A3(H2) to A4(H2) and A3(H8) to A4(H8). These nOes were indeed observed in the NOESY spectrum.[29] Such efficient purine–purine stacking provides extra stabilization to this mismatched base-pair. On the other hand, C8 is displaced from the helix axis and this is shown in Figure 4. Further, T7 is also slightly off because of the enhanced base-pair twist as discussed later. As a result, the C8(H5) and C8(H6) protons are less stacked to the flanking base-pairs (T7 and C9). Such unstacking of C8(H5) and C8(H6) protons results in unusual down field shift of their resonances, which has been indeed observed in the ^{1}H NMR spectrum[29] (δ values for C8(H5) and C8(H6) are 6.07 and 7.89 ppm, respectively), compared to the chemical shifts of C6 (δ values for C6(H5) and C6(H6) are 5.83 and 7.74 ppm, respectively) and C9 (δ values for C9(H5) and C9(H6) are 5.66 and 7.65 ppm, respectively) present in the molecular system.

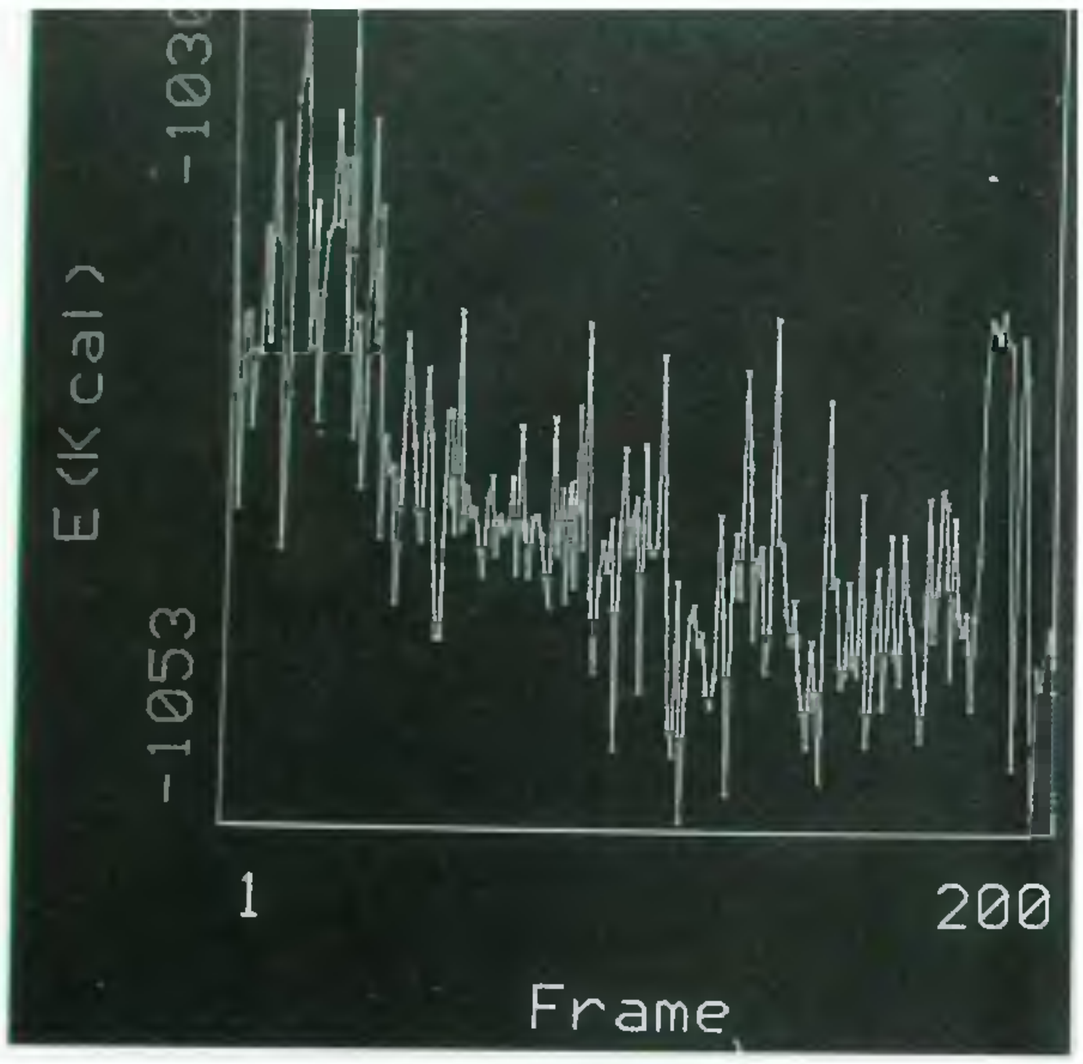

Figure 2. The plot of total energy vs. duplex structures obtained after molecular dynamics and energy minimizations.

The backbone torsion angles of the duplex are listed in Table 1. Although this duplex contains A^+–C mispair, the torsion angles, α, β, γ and ε are effectively locked into *gauche*$^-$, *trans*, *gauche*$^+$ and *trans* conformations, respectively, similar to those observed in B–DNA. The torsion angles, δ adopt 135° on an average. All the glycosyl torsion angles, χ (O4–C1′–N1–C6 for pyrimidine and O4–C1′–N9–C8 for purine), adopt *anti* conforma-

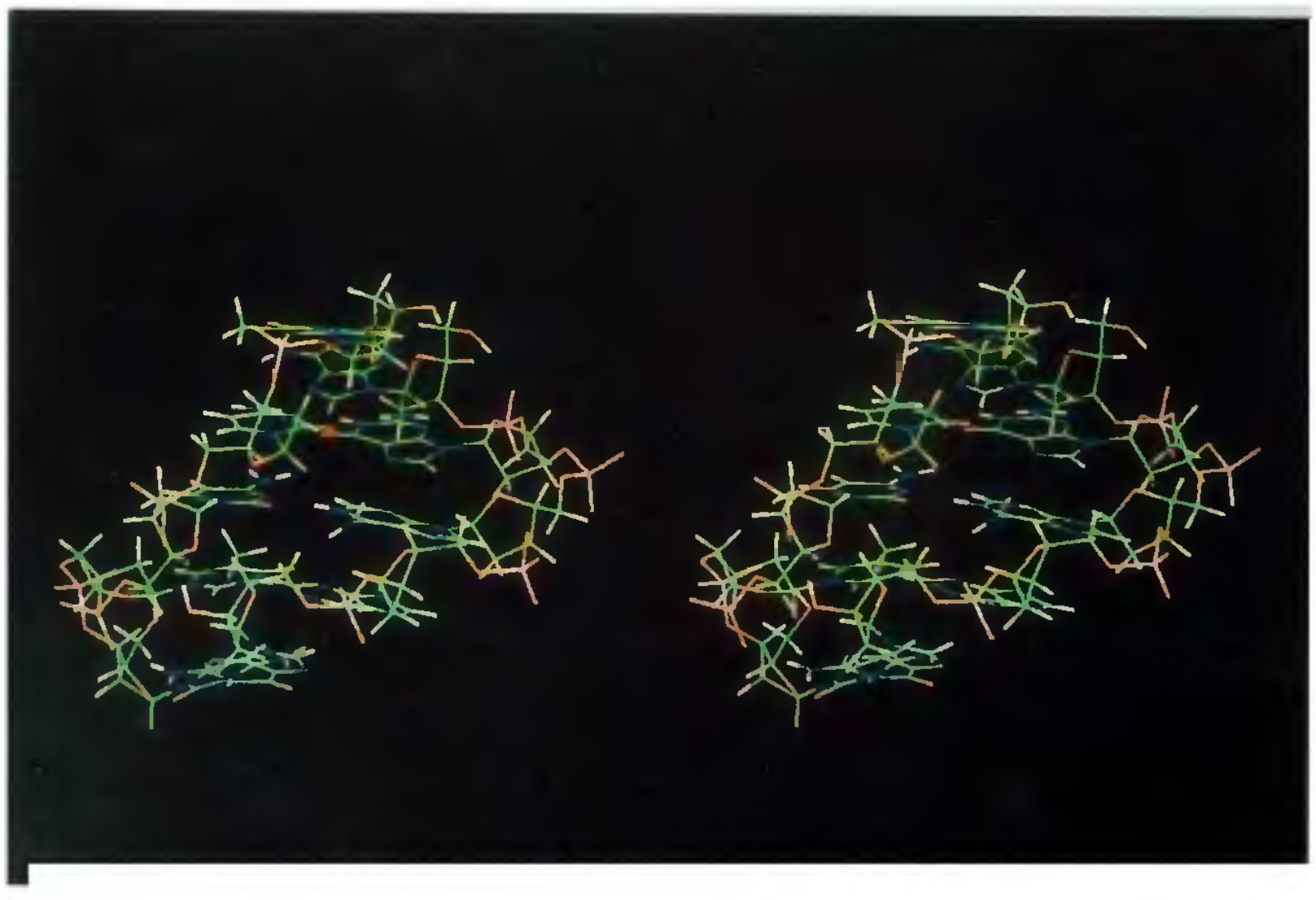

Figure 3. The stereo views of the duplex structure with lowest energy on the simulation trajectory.

tions. In addition, the C1′–C1′ distances are unaffected even in the presence of A^+–C mispair and these distances are similar to those observed in usual B–DNA.

The local base-pair roll and twist have significant structural effects. Table 2 lists local base-pair roll and twist of the duplex. There is a large positive roll for the base sequence C8–C9 (13.22) and C9–T10 (10.77) compared to the rest of the duplex. Such large positive roll angles lead to closing the major groove, which in turn leads to a sharp kinking in the direction of the major groove at C8–C9 and C9–T10, i.e. at the neighborhood of A^+–C mismatched base pair site. Further, the formation of A^+–C mispair increases the twist angle (44°) for A4:T7 base-pair (Table 3) while others are about 28° on average. As a result, T7 is slightly off with enhanced base-pair twist (Figure 4). In addition, C8 is significantly displaced from the helix axis (Table 3). It might be the reason for the nonobservance of the expected nOe interaction between H6 protons of T7 and C8 in the NOESY spectrum[29]. However, the energy related to the stacking of bases in the duplex is not

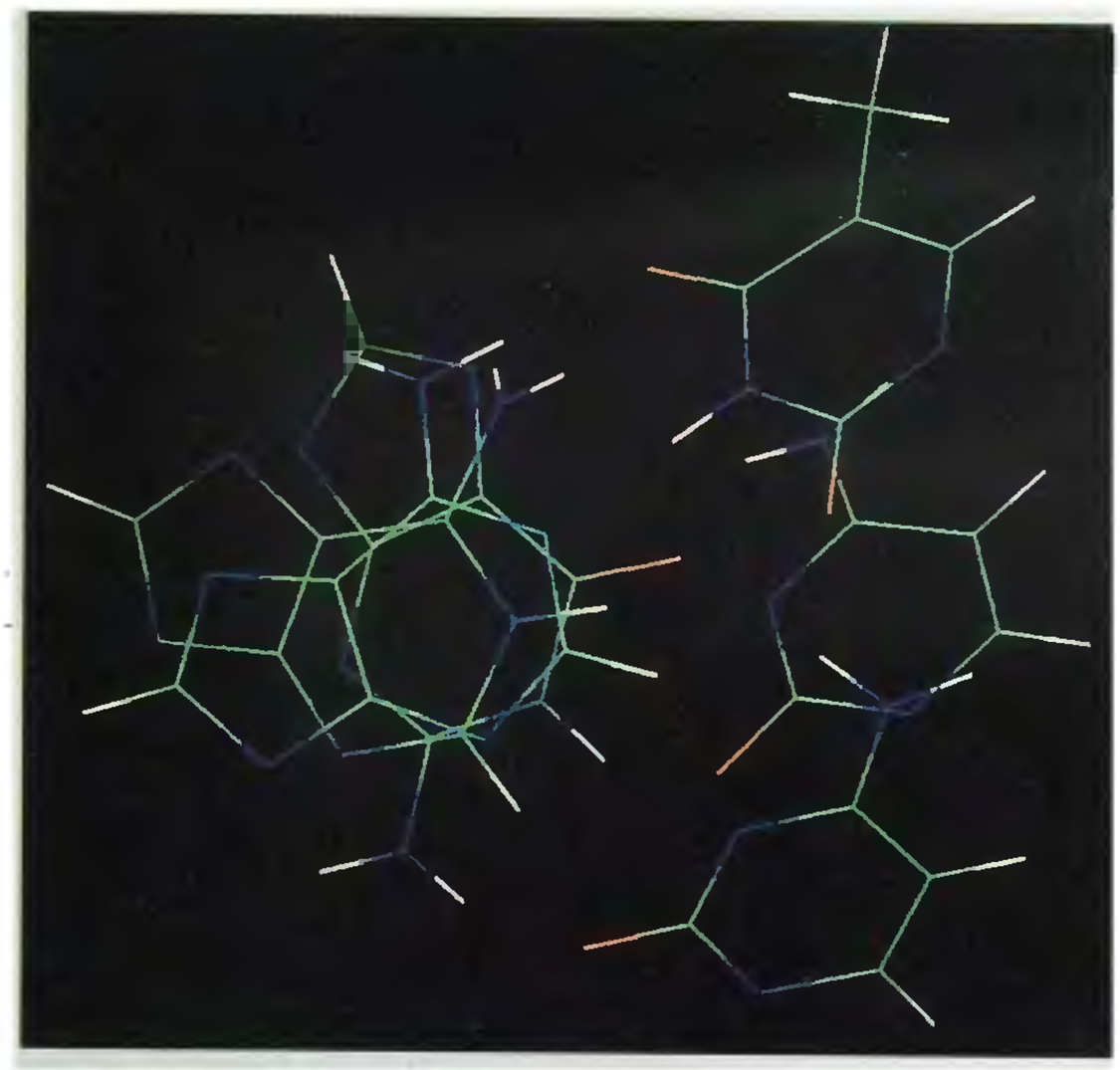

Figure 4. The superimposition of the mismatched A^+3–C8 base-pair with the flanking A4:T7 and G2:C9 base-pairs. The view is down the helix axis.

Table 1. The backbone torsional angles (in degrees) for the antiparallel DNA duplex with A^+–C mismatched base-pair

Residues	α	β	γ	δ	ε	ξ	χ
A1	–	–	57	136	–174	–102	56
G2	–73	177	57	135	179	–107	59
A^+3	–66	–167	48	138	180	–98	63
A4	–67	176	62	131	179	–106	62
G5	–66	–180	54	137	–	–	58
C6	–	–	56	136	–175	–100	50
T7	–72	–177	55	135	–177	–115	64
C8	–69	176	60	142	–178	–115	68
C9	–69	177	59	139	178	–102	58
T10	–65	–178	55	135	–	–	55

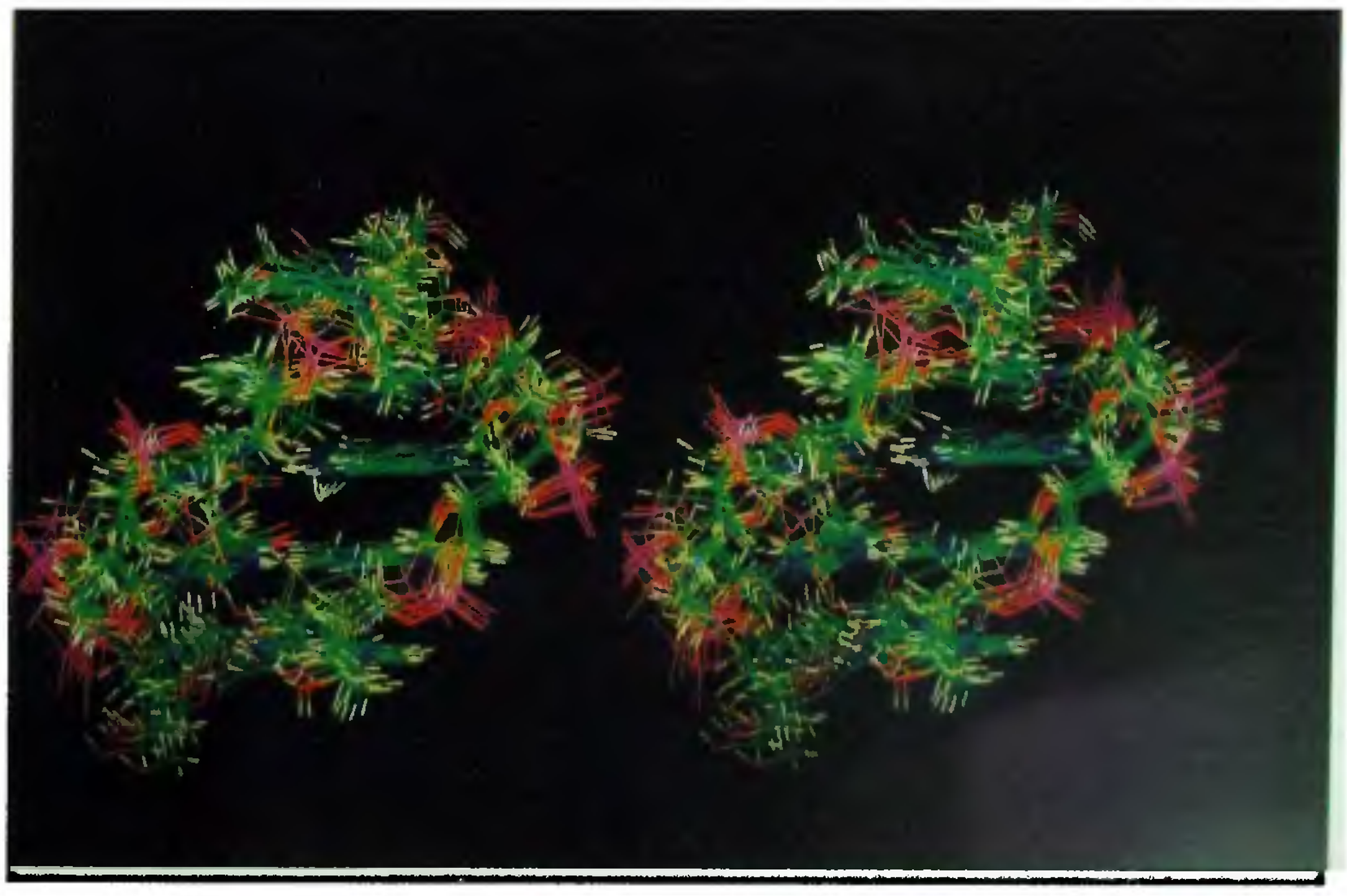

Figure 5. The superimposition of 195 ps structure on another 10 structures which lie within 2.5 kcals above the 195 ps structure on simulation trajectory.

Table 2. The local base-pair roll and twist of the antiparallel DNA duplex with A^+–C mismatched base-pair

Bases	Roll	Twist
C6:G5		
	2.12	28
T7:A4		
	2.15	44
C8–A^+3		
	13.22	25
C9:G2		
	10.77	30
T10:A1		

Table 3. X-displacement of the individual bases in the antiparallel DNA duplex with A^+–C mismatched base-pair

Bases	X-displacement (Å)
A1	–1.63
G2	–2.01
A^+3	–2.56
A4	–1.01
G5	–1.02
C6	–1.41
T7	–1.06
C8	–0.16
C9	–1.47
T10	–1.64

significantly affected and it is uniform (about 12 kcals/mole on an average) all along the duplex.

The aforementioned structure is a snapshot taken at 195 ps of the MD simulation. The other 10 structures (at 93, 106, 107, 110, 120, 139, 142, 153, 165 and 189 ps), which lie within 2.5 kcals above that of 195 ps structure (Figure 2), are superimposed on 195 ps structure and shown in Figure 5. All these superimposed structures are convergent and there is no structural diversity at or near the mismatch site.

Thus this study provides the conformational rationale of the formation of A^+–C mismatched base-pair at neutral pH.

1. Steitz, T. A., Beeze, L., Freemont, P. S., Friedman, J. M. and Sanderson, M. R., *Cold Spring Harbor Symp. Quant. Biol.*, 1987, **52**, 465.
2. Kramer, B., Kramer, W., and Fritz, H. J., *Cell*, 1984, **38**, 879–887.
3. Fazakerly, G. V., Quignard, E., Woisard, A., Guischlbauer, W., van der Marcel, G. A., van Boom, J. H., Jones, M. and Radman, M., *EMBO J.*, 1986, **13**, 3697–3703.
4. Ferbst, A. R., Knill-Jones, J. W., and Tai, W. C., *J. Mol. Biol.*, 1982, **156**, 37–51.
5. Greene, K. L., Jones, R. L., Li, Y., Robinson, H., Wang, A. H. J., Zon, G. and Wilson, W. D., *Biochemistry*, 1994, **33**, 1053–1062.
6. Chary, K. V. R., Khan, K. K., Rastogi, V. K., Govil, G., Howard, F. B. and Miles, H. T., *J. Phys. Chem.*, 1994, **98**, 9119–9125.
7. Cheng, J., Chou, S. and Reid, B. R., *J. Mol. Biol.*, 1992, **228**, 1037–1041.
8. Maskos, K., Gunn, B. M., Le Blanc, D. A., and Morden, K. M., *Biochemistry*, 1993, **32**, 3583–3595.
9. Rastogi, V. K., Chary, K. V. R., Govil, G., Howard, F. B. and Miles, H. T., *Appl. Magn. Reson.*, 1994, **7**, 1–19.
10. Brown, T., Leonard, G. A., Booth, E. D. and Chambers, J., *J. Mol. Biol.*, 1989, **207**, 455–457.
11. Gao, X. and Patel, D. J., *J. Am. Chem. Soc.*, 1988, **110**, 5178–5182.
12. Hunter, W., Brown, W. and Kennard, O., *J. Biomol. Struct. Dyn.*, 1986, **4**, 173–191.
13. Sau, A. K., Chary, K. V. R., Govil, G., Chen, C., Howard, F. B. and Miles, H. T., *FEBS Lett.*, 1995, **377**, 301–305.
14. Chou, S. H., Cheng, J. W. and Reid, B. R., *J. Mol. Biol.*, 1992, **228**, 138–155.
15. Prive, G. G., Heinemann, U., Chandrasegaran, S., Kan , L. S., Kopka, L., Dickerson, R. E., *Science*, 1987, **238**, 498–504.
16. Kan, L.-S., Chandrasegaran, S., Pulford, S. M. and Miller, P. S., *Proc. Natl. Acad. Sci. USA*, 1983, **80**, 4263–4265.
17. Nikonowicz, E. P. and Gorenstein, D. G., *Biochemistry*, 1990, **29**, 8845–8858.
18. Li Y., Zon, G. and Wilson W. D., *Proc. Natl. Acad. Sci. USA*, 1991, **88**, 26–30.
19. Patel, D. J., Kozlowski, S. A., Ikuta, S. and Itakura, K., *Federation Proc.*, 1984, **43**, 2663–2670.
20. Moe, J. G. and Russu, I. M., *Biochemistry*, 1992, **31**, 8421–8428.
21. Hunter, W. N., Brown, T., Kneale, G., Anand, N. N., Ravinovich, D. and Kennard, O., *J. Biol. Chem.*, 1987, **262**, 9962–9970.
22. Kalnik, M. W., Kouchakdjian, M., Li, B. F. L., Swann, P. F. and Patel, D. J., *Biochemistry*, 1988, **27**, 108–115.
23. Patel, D. J., Kozlowski, S. A., Marky, L. A., Rice, J. A., Broka, C., Dallas, J., Itakura, K. and Breslauer, K., *Biochemistry* , 1988, **21**, 437–444.
24. Hare, D., Shapiro, L. and Patel, D. J., *Biochemistry*, 1986, **25**, 7445–7456.
25. Hunter, W. N., Brown, T., Anand, N. N. and Kennard, O., *Nature*, 1986, **320**, 552–555.
26. Kalnik, M. W., Kouchakdjian, M., Li, B. F. L., Swann, P. F. and Patel, D. J., *Biochemistry*, 1988, **27**, 100–108.
27. Patel, D. J., Kozlowski, S. A., Ikuta, S. and Itakura, K., *Biochemistry*, 1984, **23**, 3218–3226.
28. Gao, X. and Patel, D. J., *J. Biol. Chem.*, 1987, **262**, 16973–16984.
29. Bhaumik, S. R., Chary, K. V. R., Govil, G., Liu, K. and Miles, H. T., *Biopolymers*, 1997 (in press).

ACKNOWLEDGEMENTS. Helpful discussions with Prof. G. Govil and the facilities provided by the National Facility for High Field NMR supported by the Department of Science and Technology, Department of Biotechnology, Council of Scientific and Industrial Research, Government of India, and Tata Institute of Fundamental Research, Bombay, are gratefully acknowledged.

Received 3 April 1997; revised accepted 24 March 1998